American Journal of Science, Engineering and Technology
2023; 8(1): 54-62
http://www.sciencepublishinggroup.com/j/ajset
doi: 10.11648/j.ajset.20230801.16
ISSN: 2578-8345 (Print); ISSN: 2578-8353 (Online)

Structural and Distribution of Impurities in the Fouling in Wet-Process Phosphoric Acid at T = 80°C

Yaktine Elyamani[1], Mohamed EL Guendouzi[1, *], Abdellah Elmchaouri[2], Mohamed Azaroual[3]

[1]Laboratory of Chemistry-Physics, Materials & Catalysis, Faculty Sciences Ben Msik, University Hassan II-Casablanca, Casablanca, Morocco

[2]Laboratory of Physical Chemistry and Bioorganic Chemistry, Faculty Science and Technology, University Hassan II-Casablanca, Mohammedia, Morocco

[3]CNRS/INSU - BRGM, University of Orléans, Institute of Earth Sciences of Orléans, Orléans, France

Email address:

elguendouzi@yahoo.fr (Mohamed EL Guendouzi)

[*]Corresponding author

To cite this article:

Yaktine Elyamani, Mohamed EL Guendouzi, Abdellah Elmchaouri, Mohamed Azaroual. Structural and Distribution of Impurities in the Fouling in Wet-Process Phosphoric Acid at T = 80°C. *American Journal of Science, Engineering and Technology*. Vol. 8, No. 1, 2023, pp. 54-62. doi: 10.11648/j.ajset.20230801.16

Received: January 25, 2023; **Accepted**: February 27, 2023; **Published**: March 9, 2023

Abstract: In this investigation, the mineral deposits formed in the digestion step in wet phosphoric acid production were studied. The mineralogical characterization of the fouling precipitates obtained at the temperature 80°C from the digestion step in 16-monthly production cycle was carried out. Observing successive layers, based on their colors, allowed us to distinguish fouling layers. Detailed structural aspects, and subsequently, chemical and physical properties of the fouling were determined using complementary analytical and characterization techniques. Particle size fractionation was then used to gain each fouling layer sample homogenized on the micro-scale (63µm). The major elements in the fouling were determined to be silica (Si_2O) and sodium (Na). Some chemical elements of major impurities, as well as traces, K, Al, Mg, Fe, Cu, and Zn, were detected using XRF which cannot appear in their proper solid phases. The obtained solid phases in different fouling layers are principally composed of the malladrite and gypsum minerals. The distribution of impurities into the present structures was investigated. Indeed, the mesh parameters of malladrite in the fouling layers were calculated and compared with those of the pure phase, and a good concordance is obtained. The FT-IR spectra confirm the presence of mallardite and gypsum phases and reveal a supplementary band that has been assigned to C-O vibrations in acids, esters, or ethers. The appearance of this band indicates the possible presence of organic matter within the fouling layer.

Keywords: Phosphoric Acid Wet-Process, Fouling Layer, Characterization, Impurities, Mallardite, Gypsum, Organic Matter

1. Introduction

During the process of manufacturing phosphoric acid, the fluoride is partially released within the gas streams in the form of HF and SiF_4. It is partitioned between the other phases depending on the process, the thermodynamic conditions and the quality of phosphate [1-3]. In the case of the dihydrate process, the fluoride is contained not only in the gypsum but also in the rest accompanying the phosphoric acid produced. The fluoride scale deposits are formed by reaction and complexation of fluoride with the dissolved ions contained in the aqueous phase, including sodium, potassium, magnesium, calcium, aluminum, silica [4, 5]. The fouling in reactors and production circuits is one of the major problems facing the phosphate industry [6-10]. Indeed, fouling provokes a loss of production due to the stoppages necessary to wash and clean the equipment of the production plant. These deposits are also a source of consumption of water [11-14].

The resolution of fouling problems encountered in the production of phosphoric acid are areas of applied research of great interest to the phosphate industry. Indeed, it contributes to better and sustainable management of production facilities allowing the maintenance of high production of phosphoric acid. Fouling is usually a crystalline deposit caused by the growth of mineral crystals on the surface, principally the

calcium sulphate and fluoride salts. The deposition of calcium sulfate has been the subject of numerous investigations [15-17]. However, the knowledge of the physico-chemical properties of the mineral deposits allows a better understanding of the mechanisms governing such complex thermodynamic equilibrium and reaction paths, by controlling the processes in the various and sensitive steps [18]. The characterization of the sample fouling is essential to the knowledge of the phenomena governing the deposit formation.

The formed deposits during a production cycle in the digestion step in wet phosphoric acid production of 28% P_2O_5 at a temperature of 80°C were investigated. The main objectives are to evaluate the chemical elements and their proper solid phases in the fouling, and to examine the distribution of impurities into the solid deposits. On the other hand, the key processes governing the formation of these undesirable compounds within mixtures of industrial phosphoric acid were also identified.

2. Experimental Section

2.1. Fouling Samples

The most widely used industrial phosphoric acid production technology is the dihydrate process, despite its drawbacks, including relatively low acid concentration and higher downstream energy consumption. Indeed, no quality requirement for phosphate rock is requested, low-temperature operating, infrequent maintenance, simple start-up and shutdown operation, and easy upgradability [1, 19] (Figure 1).

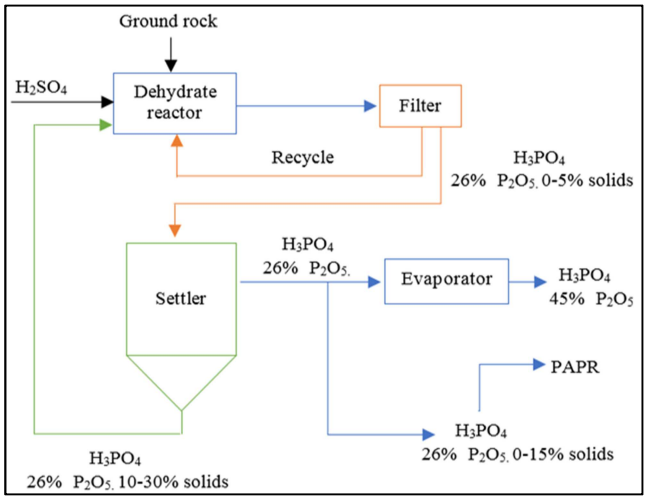

Figure 1. *Wet phosphoric acid process.*

During the filtration to concentrate the phosphoric acid, the deposits solids were precipitated. The fouling was formed during a production cycle of 16 months and appears as fouling layers that cover the entire inner surface in the digestion step (Figure 2), these deposits penalize the phosphoric acid production. The knowledge of the mineralogical characteristics of these solid phases makes it possible to understand the mechanisms governing the complex thermodynamic equilibrium and the successive reactions paths of the system.

Figure 2. *Fouling sample from the digestion step of phosphoric acid in wet phosphoric acid process.*

The characterization of most studies on deposits has been effectuated on bulk analysis, in which the structural features and the compositional profiles of layered deposits have been neglected. The present study is based on the full characterization of the compositional profile of fouling obtained during the production of phosphoric acid. The fouling layers are taken in the step of the process in the digestion of phosphoric acid of 28% P_2O_5 at the temperature of 80°C. The characteristics of the studied fouling sample are given in Table 1. Then, the particle size fractionation was employed to elaborate the fouling sample on the micro-scale.

Table 1. *Information of the fouling sample.*

Fouling sample	State	Mass	Thickness	Length	Width
	Solid	5.50 kg	6.20 cm	11.70 cm	8.80 cm

2.2. Methods and Procedures

The fouling sample was prepared on the micro-scale using particle size fractionation. Different analysis techniques were used to characterize and identify the mineral deposits, and elemental analyses were also performed.

The density of powders was measured using the pycnometer method. For solids, pycnometers of various shapes and known volumes could be used. The density is evaluated by the difference between the weight of the full and empty pycnometer, which it has a known volume. The determination of the volume of powders or granules was generally made by performing three weighings and using bi-distilled water of known density [20].

The X-ray diffraction patterns were recorded using a Brucker AXSD8 Advanced diffractometer with Cu Kα radiation (λCu, Kα=1.541874 Å). The analysis element is determined by fluorescence (XRF) spectroscopy with ICP MES Varian, S/13/35, SRS 200. The infrared (IR) spectra were collected by a Fourier transform infrared spectrometer (Shimadzu FTIR 8400). The powder samples were diluted with dry KBr (10% by weight) and front packed into the sample cell. Scanning electron microscopy (SEM) (Hirox SH 4000M) is also used to determine the morphology of the fouling sample. Different techniques were combined to know

and understand the behavior of the fouling in the digestion step in wet phosphoric acid.

3. Results and Discussions

3.1. Particle Size Fractionation of the Fouling Layers

3.1.1. Treatment of the Fouling Sample

According to the receipt of the sample at the laboratory, it needs a preliminary treatment of the fouling rock (Figure 2). At first naturally, it requires a water wash for dust removal, and separation of clogging rock per slide from the Saws cut-off for a visual mineralogy feature, to develop a fouling sample treatment protocol (Figure 3). Sampling aims at obtaining a representative fraction of a whole. Problems are encountered in the case of particulate solids that show constitution and distribution heterogeneity.

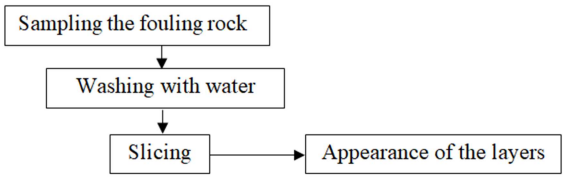

Figure 3. *Treatment Protocol of the fouling sample.*

3.1.2. Practice of Sampling

The preparation of the fouling sample includes all the steps performed in the laboratory to make a sample in a form suitable for chemical analysis. Proper sample preparation generates sub-samples representative of the entire sample. In this case, the fouling samples were taken and a visual analysis was performed to separate the fouling layers (Figure 4a), based on the appearance of different colors in the fouling sample. The fouling layers (A, B, C, and D) were then crushed and milled independently. Total dirt samples (about 300g) obtained from each layer were dried in the air, weighed and then sieved to dryness using a sieve (square mesh of 2mm, surface 1m^2) (Figure 4b). The analysis indicated considerable homogeneity on the micro-scale, compounding the heterogeneity of bulk scale composition. Indeed, dry sieving was made on series of sieves for dimensions between 25mm and 63µm. The sieving time is limited to 15 min, the sieves need continuous vibrations. The usual wire cloths which fill the sieves have opening diameters (mesh sieves 1mm) whose succession is based on a logarithmic geometric progression. Several standards are very similar. The most widespread classification of particle sizes of the fouling sample is the standard NF P 94-057 [21], which defines grain size classes in soils.

The resolution of the result depends on the number of sieves used. The column can be composed of 16 to more than 20 screens of apertures ranging from 25 mm to 63µm. The particle size distribution of the fouling particles influences the chemical physic properties of the solids. Therefore, it is important to be able to monitor and control the quality of powders and granules. Figure 5 shows SEM images of the surface morphology of the fouling layer samples (A, B, C, and D).

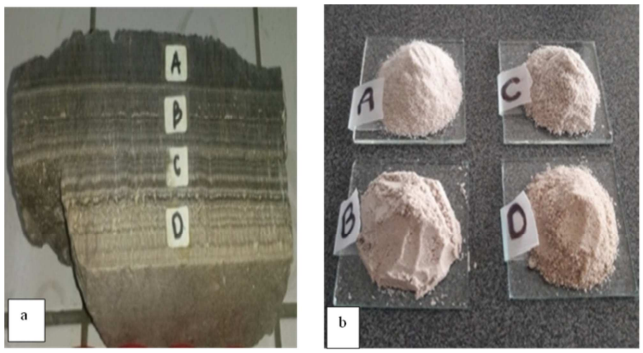

Figure 4. *Macroscopic images of the fouling layers (a) and the sample fractions (b).*

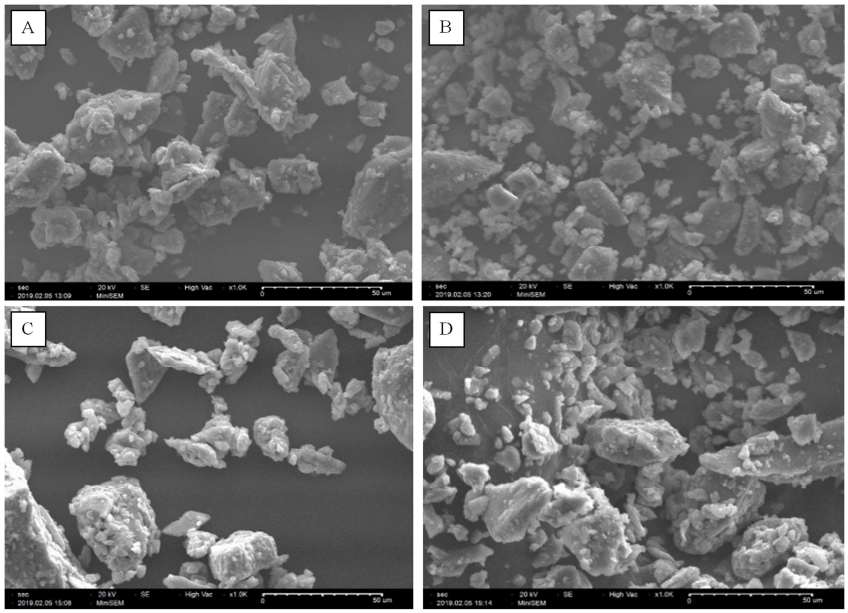

Figure 5. *SEM images of the samples of fouling layers.*

3.2. Characterization of the Fouling Layer Samples

The analytical techniques were employed to explore detailed structural aspects, and subsequently, chemical and physical properties of the fouling layer sample. Elemental analyses and the density of the samples were carried out, and the samples were characterized using XRD, XRF, and FT-IR.

Density measurements

The density is a fundamental physical property of rocks in various areas such as the geological and mining industry. Therefore, the density measurements of fouling samples are a significant investigation in the phosphate industry and geo-engineering. The difference between the weight of the full and empty pycnometer, with the known volume, allows us to determine de density. The apparent density of the sample's fouling layers, A, B, C, and D was measured using a pycnometer method at the temperature of 25°C with the uncertainty $u(d)$ = 0.0001 (Figure 6). The average density of the fouling samples owns a value of 2.6223. The density decreases from the fouling layer A to D, and follows this order $d_A > d_B > d_C > d_D$ (inner, hung on the surface of the digester) to D (outer). The behavior is conditioned by the agitation and the temperature gradient effect during the digestion step in wet process phosphoric acid. The density of the fouling layers could be explained by different weight compounds and matter in each layer.

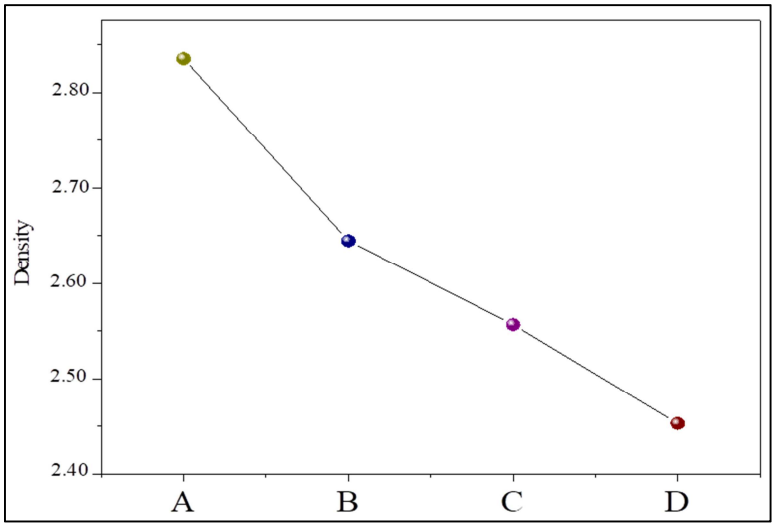

Figure 6. *Density of the fouling samples at T=25°C.*

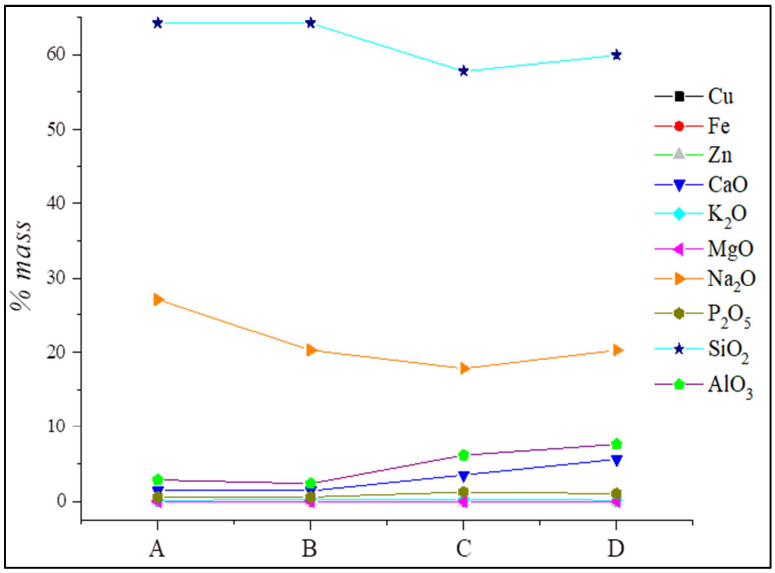

Figure 7. *Chemical analysis of the fouling layers.*

X-ray fluorescence

The elemental analysis was performed for the fouling layer samples using X-ray fluorescence (Table 2, Figure 7). According to figure 7, the major elements in the samples were determined to be silica (Si_2O) and sodium (Na). Moreover, Si_2O was also found in large quantities in silicates. Na appears in much greater proportions in the fouling layers. The fouling layers show more similarities in terms of

elementary compositions, but with different proportions.

Table 2. *Distribution of impurities in the fouling layer.*

Element analysis in fouling layer (% mass)	CaO	K_2O	Na_2O	P_2O_5	SiO_2	Al_2O_3
A	1.40	0.12	27.00	0.57	64.22	2.84
B	1.41	0.30	20.25	0.58	64.20	2.36
C	3.50	0.24	17.82	1.26	57.78	6.14
D	5.60	0.18	20.25	1.03	59.92	7.56

Standard uncertainty is u= 0.01

The amount of some elements decreases slightly in the fouling layers, in contrast, the others remained practically constant in all samples, including K, Al, Mg, Fe, Cu, and Zn. Indeed, the phosphate ore is represented mainly by fluoroapatite $[Ca_3(PO_4)_2]_3CaF_2.CaCO_{3(s)}$ with some additional compounds. Wet process using sulphuric acid is the most common means of producing phosphoric acid. The simplified overall phosphate rock attack is given by reaction (1),

$$Ca_3(PO_4)_{2(s)} + 3\,H_2SO_{4\,(l)} + 3nH_2O_{(l)} \rightarrow 2\,H_3PO_{4(l)} + 3\,CaSO_{4(s)}.nH_2O \quad (1)$$

where n is 0, 1/2 or 2. Depending on physico-chemical and thermodynamic conditions, the calcium sulphate can precipitate as the anhydrite, hemihydrate or dihydrate (gypsum). All these allotropic solid phases have very low solubilities.

In the phosphate rocks from sedimentary origin, the fluorine content varies between 3 and 4%. During wet-process production of phosphoric acid, the fluorine can be released with the gaseous streams in the form of HF and SiF_4 [22] or inserted in form of solid phases with gypsum. The remaining fraction is solubilized in the phosphoric acid product. The fluorine content remains in the same order of magnitude as in the original phosphate rocks. The silica content has an average value of 3.67% SiO_2 [19]. In phosphate leaching processes, it combines with other impurities contained in the aqueous phase (phosphoric acid) to give rise to other solid-aqueous chemical species, damaging and penalizing the process [18, 23].

X-ray diffraction studies

To characterize and identify the obtained solid phases contained in different fouling layers, the X-ray diffraction analysis has been done using the source of Cu-K_α (wavelength 1.541874 Å). The diffractograms of the fouling layer samples were given in Figure 8. Comparing the peaks of experimental data with those contained in a known database makes it possible to identify unknown materials [24-27]. The observed diffraction peaks were attributed to those of the malladrite form (Na_2SiF_6) in all samples A-D. According to the diffractograms, the crystalline form of gypsum ($CaSO_4.2H_2O$) was also observed. The obtained results show the appearance of mallardite form with the decreasing of the peak intensity from the samples fouling layer A to D. However, the peak of gypsum at 2θ=12 decreases considerably in layer A.

FT-IR spectroscopy

The FT-IR spectra of the samples (A- D) show some functional groups, (Figure 9). IR spectra can be expressed in bands at 3448 cm^{-1}, the elongation bands of the main O-H groups. The intense bands observed at 733 cm^{-1} and 477-496 cm^{-1} have been assigned as Si–F stretching vibrations, which is the main character of Na_2SiF_6 [28].

The band at 603 cm^{-1} attributes at the elongation SO_4 which corresponds to gypsum ($CaSO_4.2\ H_2O$) [26, 29]. The appearance of the band at 1130-1134 cm^{-1} has been assigned to C-O as vibrations in acids, esters, or ethers [30, 31], and revealed the possibility of the presence of organic matter in the fouling layer. This band intensity increases from sample A to D, and the IR spectra are very similar, which means that they were formed by the same type of functional groups. The complementary analytical techniques were used to illustrate the identification and characterization of the fouling layers A-D. They reveal the compounds of malladrite, gypsum, trace metals, and the possibility of the presence of organic matter.

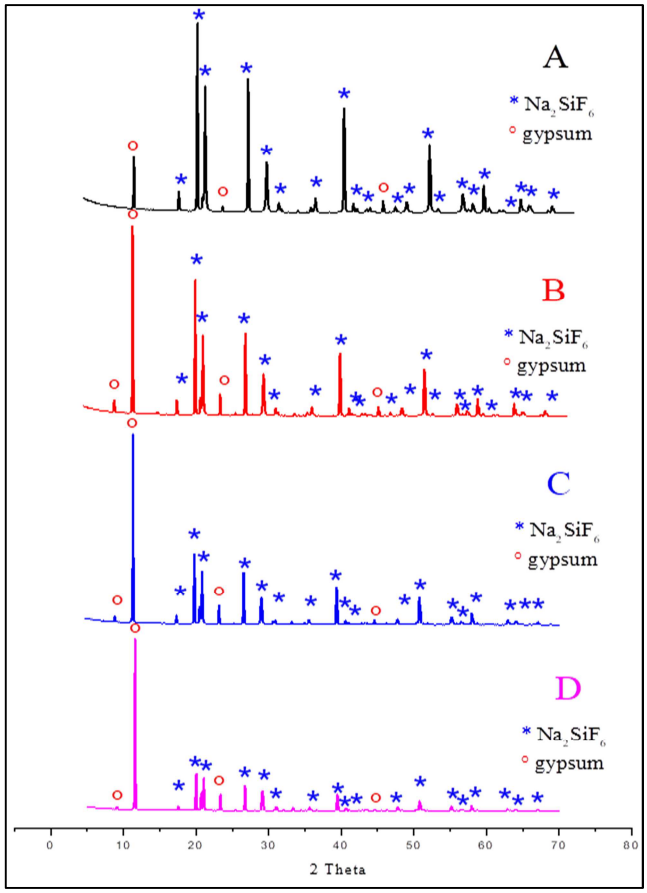

Figure 8. *Diffractograms of the fouling layer samples (A, B, C, and D).*

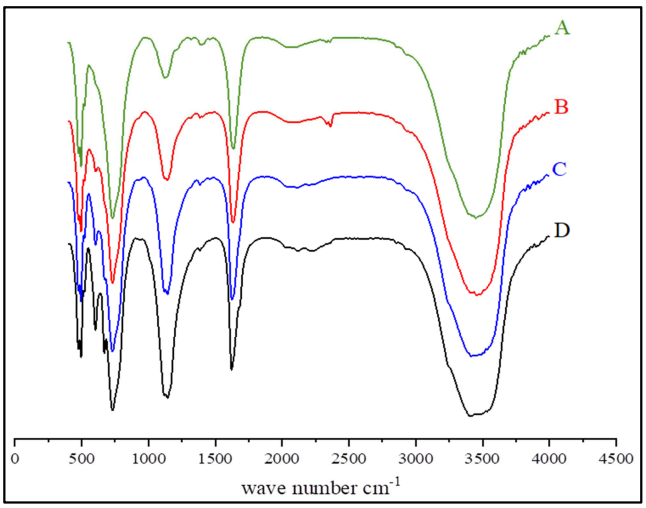

Figure 9. *Infrared spectra of the samples fouling.*

3.3. Impurities and Malladrite Structure

Precipitate of mallardite form

The obtained results (Figure 8) show an absolute predominance of the mallardite form with the decreasing of the peak intensity from the samples fouling layer A to D. The chemical elements detected by XRF (Figure 7) such as Si (SiO_2) and sodium (NaO_2) with high concentration were appeared in malladrite form, formed according to the eq. 4. Indeed, during the production of phosphoric acid, the gypsum or fluorosilicate salts precipitations generate fouling problems (eqs. 2-4). The hexafluorosilicate salts are combined with other impurities to give birth to other aqueous and solid chemical species in the aqueous phase.

The attack of fluophosphocarbonate complex with the sulfuric acid is given by the reaction (eq. 2):

$$[Ca_3(PO_4)_2]_3CaF_2.CaCO_{3(s)} + 11\ H_2SO_{4(l)} + 21H_2O_{(g)} \rightarrow 11\ CaSO_{4(s)}.2\ H_2O + 6\ H_3PO_{4(l)} + 2\ HF_{(g)} + CO_{2(g)} \quad (2)$$

The presence of excess impurities such as silica in the phosphoric acid could induce ancillary reactions with hydrofluoric acid giving potentially either silicon tetrafluoride or fluosilicic acid (eq. 3):

$$6\ HF_{(aq)} + SiO_{2(s)} \leftrightarrow H_2SiF_{6(aq)} + 2\ H_2O_{(l)} \quad (3)$$

The distribution of fluorine in the phosphoric acid and the gypsum depends on the SiO_2/ F and Na_2O/ F ratios in the phosphate. Na_2O or K_2O reacts with H_2SiF_6 (eq. 4):

$$H_2SiF_{6(l)} + Na_2O_{(s)} \leftrightarrow Na_2SiF_{6(s)} \downarrow + H_2O_{(l)} \quad (4)$$

In this case, the solubility of each mineral depends on the molality range of phosphoric acid and that of involved species in the aqueous solutions at a temperature of 80°C. The aqueous phase is composed of the concentrated phosphoric acid solution of 28% P_2O_5, with a value of pH equals to -0.65 and low water activity (a_w=0.5400) [32]. The diagnosis of the risk of fouling requires a knowledge of the optimal conditions for the solubility of concerned minerals in the phosphoric acid solutions. However, the solubility of mallardite in aqueous solutions is principally conditioned by the thermodynamic equilibrium state of the system at a given temperature [25]. In the condition of wet-process of phosphoric acid, the Si, Na, Ca and SO_4 concentrations (Figure 7) are sufficiently high in an acidic solution (28% P_2O_5, low pH) at *T*=80°C to induce the precipitation of mallardite and also gypsum.

Distribution of impurities

Some chemical elements of major impurities were identified using XRF, as well as traces, K, Al, Mg, Fe, Cu, and Zn. These elements cannot appear in proper solid phases (Figure 8). They could be inserted into the present structures of malladrite and/or gypsum. Indeed, numerous studies have shown the impurities effects on the crystallization of calcium sulphate [33-36]. The effects of gypsum precipitation in the presence of cationic and anionic impurities in aqueous brine have been reported [33]. Impurities in phosphate rock have an effect on the crystal form of gypsum crystallinity during the production of wet phosphoric acid and shown that the crystal form of gypsum changes little in the presence of Al^{3+} [34-36]. Other effect, they can catalyze the gypsum precipitation, with iron and potassium show the greatest effect.

Furthermore, some impurities, as well as traces, can impact the structure of mallardite. However, the insertion of the impurities into the malladrite crystal has been studied.

The peak intensity of malladrite decreases from A to D indicating that its concentration decreases accordingly; from the bottom to the top of the fouling layers. Indeed, the structure of the mallardite is hexagonal and crystallizes in space group P321. The "SiF_6" groups are almost regular octahedral with a Si-F distance of 1.695Å [24, 37]. The Miller index hkl was calculated for all peaks and deducted the parameters of mesh as a = 8.859Å, c = 5.038Å (± 0.002 Å) (Figure 10).

The comparison was made between the calculated mesh parameters of the malladrite in the fouling layers and those of the pure phase [24]; and showed a good agreement with the same values. So, the impurities should be not included in the crystal structure of malladrite. However, the positions of the peaks inform us about the network; Miller indices, symmetries, parameters of mesh, and often a group of space. To access the atomic positions, the relative intensities of each fouling sample A-D are used.

A diffraction pattern can be calculated by Fourier transformation, using the new set of phases generated after each cycle of refinement. As the refinement progresses, the difference between the evaluated diffraction pattern and the experimental is minimized. According to the numerical treatment of the observed positions of the peaks and their intensities, it is possible to go back to the complete structure of the malladrite molecule of the fouling layer samples. The representation is given in two forms in 2D and 3D dimensions (Figure 11).

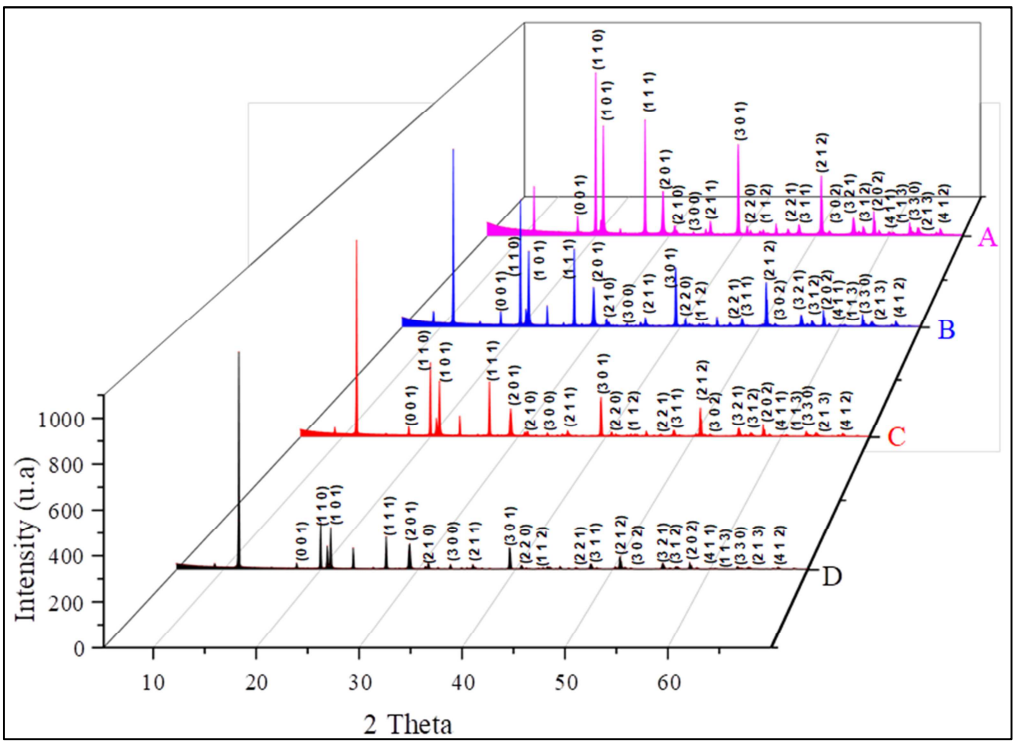

Figure 10. *Diffractograms corresponding Miller families of each fouling layer (A, B, C, and D).*

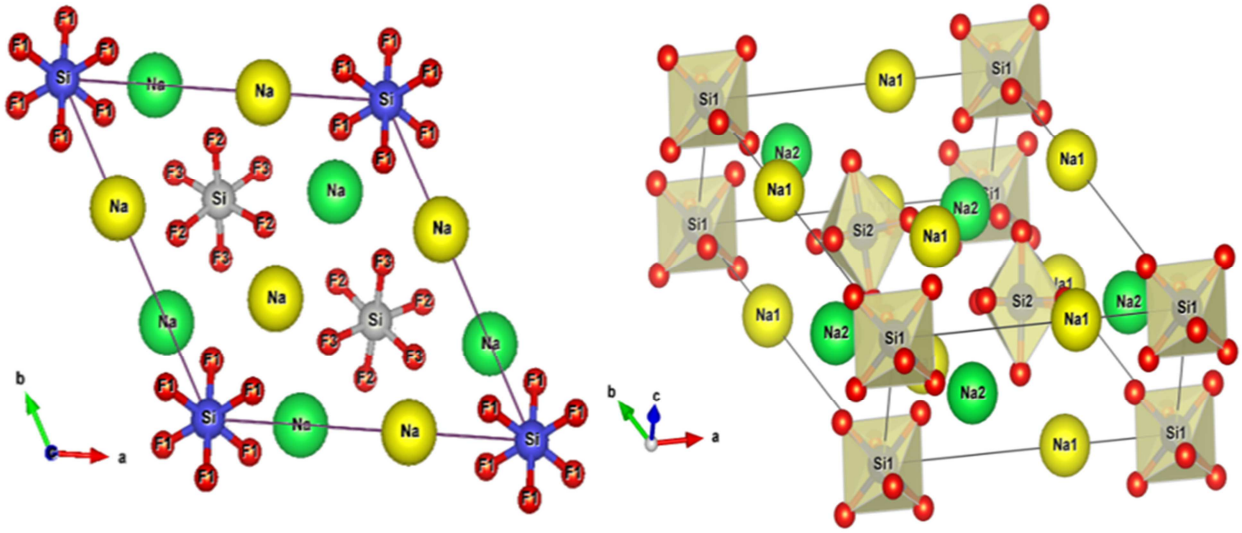

Figure 11. *Structure in 2D and 3D dimensions of the X-ray diffraction patterns of the mallardite.*

4. Conclusion

The solid deposits in the digestion step in wet phosphoric acid production of 28% P_2O_5 at *T*=80°C were studied. The fouling samples were homogenized and prepared on the micro-scale using particle size fractionation. Different colors were observed in the fouling layers and allowed a priori visual analysis of the fouling layers (A-D). The density of the fouling samples decreases from layer A to D. The characterization of the mineral deposits was made using complementary techniques XRF, XRD, IR. The obtained solid phases are principally composed of malladrite and gypsum. Some impurities were identified using XRF, as well as traces, K, Al, Mg, Fe, Cu, and Zn, and their distribution into the present structures were studied. Based on the calculated mesh parameters of malladrite in the fouling layers and the pure one, the impurities should be not included in the crystal structure of malladrite. The appearance of the band assigned to C-O vibrations (IR) reveals the presence of organic matter in the samples. This matter is the key to explaining the different colors observed in the fouling layers. The obtained results represent an important contribution to both for fundamental and industrial interests, particularly for the phosphate industry, and allow a better understanding of the mechanisms governing such complex thermodynamic equilibria.

References

[1] Becker P. Phosphates and Phosphoric Acid, Fertilizer Science and Technology Series 3, Marcel Dekker, New York; 1983.

[2] Frazier AW, Lehr JK, Dillard EF. Chemical Behaviour of Fluorine in Production of Wet Process Phosphoric Acid. Environ. Sci. Technol. 1977; 11; 1007−1014.

[3] Wu S, Wang L, Zhao L, Zhang P, El-Shall H, Moudgil B, Huang X, Zhang L. Recovery of rare earth elements from phosphate rock by hydrometallurgical processes–A critical review. Chem. Eng. J. 2018; 335; 774-800.

[4] Van Der Sluis S. A Clean Technology of Phosphoric Acid Process, Delft University Press 1987.

[5] El Yamani Y, EL Guendouzi M, El Mchaouri A. Impact of fluorine compounds on the phosphoric acid production. Proceedings RSE-2016. 2016; 1; 54-60.

[6] Behbahani RM, Müller-Steinhagen H, Jamialahmadi M. Investigation of Scale Formation in Heat Exchangers of Phosphoric Acid Evaporator Plants. Can. J. Chem. Eng. 84 (2006) 189-197.

[7] Somerscales EFC. Fouling of Heat Transfer Surfaces, an Historical Review, 25th Nat. Heat Trans. Conf. ASME, Houston; 1988.

[8] Kapustenkoa P, Boldyryeva S, Arsenyevab O, Khavinb G. The use of plate heat exchangers to improve energy efficiency in phosphoric acid production. J. Clean. Prod. 2009; 17; 951–958.

[9] Khamar L, EL Guendouzi M, Amalhay M, Aboufaris El alaoui M, Rifai A, Faridi J, Azaroual M. Evolution of soluble impurities concentrations in industrial phosphoric acid during the operations of desupersaturation. Procedia Eng. 2014; 83; 243−249.

[10] Dorozhkin VS. Fundamentals of the Wet-Process Phosphoric Acid Production. 1. Kinetics and Mechanism of the Phosphate Rock Dissolution. Ind. Eng. Chem. Res. 1996; 35; 4328−4335.

[11] Weijnen MPC, Van Rosmalen GM. The influence of various polyelectrolytes on the precipitation of gypsum. Desalination. 1985; 54; 239–261.

[12] El-Shall H, Abdel-Aal EA, Moudgil BM. Effect of Surfactants on Phosphogypsum Crystallization and Filtration during Wet-Process Phosphoric Acid Production. Sep Sci Technol. 2000; 35; 395-410.

[13] Valdez Salas B, Wiener M S, Salinas Martinez J R. Phosphoric Acid Industry: Problems and Solutions, Phosphoric Acid Industry, IntechOpen, 2017, edited by. Wiener M S, Valdez B. https://doi.org/10.5772/intechopen.70031

[14] Wang Y W, Meldrum F C. Additives stabilize calcium sulfate hemihydrate (bassanite) in solution, J. Mater. Chem., 2012; 22; 22055-22062.

[15] Amjad Z. Calcium Sulfate Dihydrate (Gypsum) Scale Formation on Heat Exchanger Surfaces: The Influence of Scale Inhibitors. J. Colloid Interface Sci. 1987; 123; 523-536.

[16] Hasson D, Zahavi J. Mechanism of Calcium Sulfate Scale Deposition on Heat Transfer Surfaces. Ind. Eng. Chem. Fundamen. 1970; 9; 1-10.

[17] Gill JS, Nancollas GH. Kinetics of growth of calcium sulfate crystals at heated metal surfaces. J. Cryst. Growth. 1980; 48; 34–40.

[18] Azaroual M, Kervevan C, Lassin A, André L, Amalhay M, Khamar L, EL Guendouzi M. Thermo-kinetic and Physico-Chemical Modeling of Processes Generating Scaling Problems in Phosphoric Acid and Fertilizers Production Industries. Procedia Eng. 2012; 46; 68−75.

[19] Murzin D Y. Chemical processes and unit operations, Berlin, Boston: De Gruyter, 2022.

[20] Franklin JA. Suggest Methods for Determining Water Content, Porosity, Density, Absorption and Related Properties and Swelling and Slake-Durability Index Properties. Int. J. Rock Mech. Min. Sci. Geomech. Abstr. 1979; 16; 141-156.

[21] Norme AFNOR P 94-057. Reconnaissance et essais - Analyse granulométrique des sols - Méthode par sédimentation. Afnor. Paris (1992). Or [20] NF EN ISO 17892-4 Janvier 2018 Reconnaissance et essais géotechniques - Essais de laboratoire sur les sols - Partie 4: Détermination de la distribution granulométrie des particules; 2018.

[22] Van Der Sluis S, AHM Schrijver, Baak FPC, Van Rosmalen GM. Fluoride Distribution Coefficients in Wet Phosphoric Acid Processes. Ind. Eng. Chem. Res. 1988; 27; 527-536.

[23] Habashi F, Awadalla F. The removal of fluorine from wet process phosphoric acid. Separ. Sci. Technol. 1983; 18; 485-491.

[24] Zalkin A. Forrester JD, Templeton DH. The crystal structure of sodium fluorosilicate Locality: synthetic. Acta Crystallogr. 1964; 17; 1408−1412.

[25] EL Guendouzi M, Skafi M, Rifai A. Hexafluorosilicate Salts in Wet Phosphoric Acid Processes: Properties of X_2SiF_6–H_2O with X = Na^+, K^+, or NH_4^+ in Aqueous Solutions at 353.15 K. J. Chem. Eng. Data 2016; 61; 1728–1734.

[26] Hass M, Sutherland GBBM. The Infra-Red Spectrum and crystal structure of gypsum. Proc. Roy. Soc. 1956; 236A; 427-445.

[27] Follner S, Wolter A, Helming K, Silber C. On the real structure of gypsum crystals. Cryst. Res. Technol. 2002; 37; 207–218.

[28] Badachhape RB, G. Hunter, McCory LD, Margrave JL. Infrared Absorption Spectra of Inorganic Solids. IV. Hexafluorosilicates. Raman Spectra of Aqueous SiF_6^{2-}. Inorg. Chem. 1966; 5; 929-931.

[29] Seidl V, Knop O, Falk M. Infrared studies of water in crystalline hydrates: gypsum, $CaSO_4.2H_2O$. Can. J. Chem. 1969; 47; 1361-1368.

[30] Springer P, Curran C. Infrared Spectra of Complexes of Metal Halides with Esters of Amino Acids. Inorg. Chem. 1963; 2; 1270-1275.

[31] Corbridge DD, Lowe EJ. Infrared spectrum of certain inorganic phosphorus compounds. J. Chem. Soc. 1954; 493-502.

[32] Khamar L, EL Guendouzi M, Amalhay M, Azaroual M. Approche expérimentale d'étude des encrassements au niveau des installations de production d'acide phosphorique. Proceedings COVAPHOS III. 2009; 5; 135-141.

[33] Budz J, Jones AG, Mullin JW. Effects of Selected Impurities on the Continuous Precipitation of Calcium Sulphate (Gypsum). J. Chem. Tech. Biotechnol. 1986; 36; 153–161.

[34] Jun L, Jian Hua W, Yun Xiang Z. Effects of the Impurities on the Habit of Gypsum in Wet-Process Phosphoric Acid. Ind. Eng. Chem. Res. 1997; 36; 2657-2661.

[35] Martynowics ETMJ, Witkamp GJ, Van Rosmalen GM. The Effect of Aluminum Fluoride on the Formation of Calcium Sulfate Hydrates. Hydrometallurgy, 1996; 41; 171-186.

[36] Kruger A, Focke WW, Kwela Z, Fowles R. Effect of Ionic Impurities on the Crystallization of Gypsum in Wet-Process Phosphoric Acid, Ind. Eng. Chem. Res. 2001; 40; 1364-1369.

[37] Schafer GF. The crystal structures of Na_2TiF_6 and Na_2SiF_6. Z. Kristallogr. 1986; 175; 269-276.